Environmental Science and Pollution Research
https://doi.org/10.1007/s11356-020-11245-6

RESEARCH ARTICLE

Microbial fuel cell soft sensor for real-time toxicity detection and monitoring

Ademola Adekunle[1] · Abraham Gomez Vidales[1] · Lyne Woodward[2] · Boris Tartakovsky[1]

Received: 16 July 2020 / Accepted: 12 October 2020

Abstract

Real-time toxicity detection and monitoring using a microbial fuel cell (MFC) is often based on observing current or voltage changes. Other methods of obtaining more information on the internal state of the MFC, such as electrochemical impedance spectroscopy (EIS), are invasive, disruptive, time consuming, and may affect long-term MFC performance. This study proposes a soft sensor approach as a non-invasive real-time method for evaluating the internal state of an MFC biosensor during toxicity monitoring. The proposed soft sensor approach is based on estimating the equivalent circuit model (ECM) parameters in real time. A flow-through MFC biosensor was operated at several combinations of carbon source (acetate) and toxicant (copper) concentrations. The ECM parameters, such as internal resistance, capacitance, and open-circuit voltage, were estimated in real time using a numerical parameter estimation procedure. The soft sensor approach proved to be an adequate replacement for EIS measurements in quantifying changes in the biosensor internal parameters. The approach also provided additional information, which could lead to earlier detection of the toxicity onset.

Keywords MFC · Biosensor · Toxicity · Online · Equivalent model, EIS

Introduction

Environmental monitoring often includes performing acute lethality tests, e.g., using daphnia or trout species. These tests are carried out in a laboratory, are infrequent due to manual sampling, and inherently laborious and time-consuming. The timely detection of toxicants in the environment is becoming increasingly important for controlling and preventing damage to ecosystems. Delays in detecting spills of toxic compounds to the ecosystem can lead to loss of biodiversity, harm human health, and, eventually, increase the cost of remediation. Therefore, recent research efforts are focused on developing real-time toxicity detection and monitoring methods (Adekunle et al. 2019b; Kholodkevich et al. 2008). Such real-time toxicity monitoring has been shown to have a wide range of possible applications in mining, agriculture, and health and food industries (Chouler and Di Lorenzo 2015; Xu and Ying 2011). Amongst real-time toxicity monitoring methods being developed, microorganism-based (biomonitoring) systems are popular due to their high sensitivity to a broad range of toxicants, fast regeneration (recovery) rates, easy maintenance, genetic homogeneity, and versatility (Cho et al. 2004; Gu et al. 1999; Lee and Gu 2005; Wu et al. 2020).

Several recent studies have demonstrated successful application of microbial electrochemical (bioelectrochemical) systems as real-time biosensors (Adekunle et al. 2019b, 2020; Chouler et al. 2018; Commault et al. 2016; Jiang et al. 2018; Pham et al. 2019; Schievano et al. 2018; Wang et al. 2018; Yu et al. 2017; Zhao et al. 2019; Zhou et al. 2018). A bioelectrochemical system (BES) consists of an anode which acts as an electron acceptor during microbial respiration and a cathode where the reduction reactions take place (Rabaey 2005). Notably, microbial fuel cells (MFCs), which are a type of BES, are often used as biosensors due to their fast response time and simple construction. Also, MFCs do not need an

Responsible editor: Philippe Garrigues

Electronic supplementary material The online version of this article (https://doi.org/10.1007/s11356-020-11245-6) contains supplementary material, which is available to authorized users.

✉ Boris Tartakovsky
Boris.Tartakovsky@cnrc-nrc.gc.ca

[1] National Research Council of Canada, 6100 Royalmount Ave, Montreal, QC H4P 2R2, Canada

[2] École de Technologie Supérieure, 1100 Notre-Dame St W, Montreal, QC H3C 1K3, Canada

Published online: 22 October 2020

external power input, as they produce rather than consume electricity (Adekunle et al. 2019a). Different designs (single or double chamber) incorporating different liquid flow patterns (flow-through, floating, capillary, etc.) were proposed for MFC-based biosensors (Adekunle et al. 2020; Choi 2015; Chouler et al. 2018; Jiang et al. 2018; Logroño et al. 2016; Zhao et al. 2019). Also, either the anode or the cathode of the MFC-based biosensors can be configured as the sensing element depending on the sensor design, analyte composition, and intended use (Zhao et al. 2019). MFC-based biosensor response to toxicity is typically observed through easily measurable outputs, such as voltage or current. Commonly, inhibition ratios calculated by the percentage drop in the voltage or current of the biosensor after the introduction of a toxicant are used to determine relative toxicity (Kim et al. 2007; Yu et al. 2017). However, several ambiguities exist due to electroactive microorganisms' sensitivity to a broad range of organic and inorganic compounds, including heavy metals, metalloids, hydrocarbons, etc. Also, MFC voltage and current response to the presence of toxic compounds tend to be delayed by several hours, especially at low (e.g., parts per billion) range of toxicant concentrations.

Soft sensors are often used for estimating process parameters, which are difficult to measure online. In our previous study, a material balance model of an MFC anodic compartment was used to improve COD (chemical oxygen demand) estimation accuracy (Recio-Garrido et al. 2017). Furthermore, a simple equivalent circuit model (ECM) of an MFC has been proposed (Coronado et al. 2013, 2015). Analysis of ECM parameters (internal resistances and capacitance) as well as direct measurements using electrochemical impedance spectroscopy (EIS) technique showed that these parameters are well correlated with the anodic liquid composition, i.e., the internal capacitance was observed to increase and the internal resistance to decrease at high concentrations of carbon source (Coronado et al. 2015; Jiang et al. 2017a; Sindhuja et al. 2016). These studies suggest that measurements of the internal parameters can be helpful in improving the sensitivity and reducing response times for toxicity detection in MFCs. Furthermore, it can be suggested that by monitoring changes in internal MFC parameters and comparing these changes with voltage and current measurements, false alarms can be prevented. Although electrochemical characterization methods are available (EIS, cyclic voltammetry, etc.), these methods are disruptive and often result in long recovery times. Thus, a non-invasive model-based estimation of MFC internal parameters is preferable. This work evaluates the suitability of an ECM-based soft sensor approach for real-time toxicity estimation by monitoring changes in the internal parameters of MFC biosensors exposed to varying concentrations of copper (Cu) as a model toxicant, and correlating these changes with Cu concentrations.

Material and methods

Stock solutions and analytical methods

A stock solution of sodium acetate 10 g L^{-1} (as $C_2H_4O_2$) was used as a carbon source. The stock solution was diluted with moderately hard water (MHW) consisting of (in mg L^{-1}): calcium (6.9), magnesium (94.5), and sodium bicarbonate (96) prepared as described in an earlier study (Adekunle et al. 2020). Different Cu concentrations were obtained by diluting a prepared Cu stock solution with the MHW.

The chemical oxygen demand (COD) of water fed to the biosensor was measured using a PeCOD® analyzer (MANTECH Inc., Guelph, ON, Canada). The concentration of Cu in the influent was measured by inductive coupled plasma mass spectrophotometry (ICP-MS), as described elsewhere (Beauchemin 2010).

Biosensor design and operation

The flow-through membraneless MFC-based biosensor consisted of an air-breathing cathode, and carbon felt anode as described in our previous study (Adekunle et al. 2019b). The anode consisted of two layers of 100 × 50 mm, 5 mm thick carbon felts (SGL Group, Charlotte, NC, USA), in a total compartment volume of 50 mL. The air-breathing manganese oxide-coated cathode (Electric Fuel Ltd., Bet Shemesh, Israel) had a dimension of 100 × 50 mm. The electrodes were separated by a 1-mm nylon cloth. Figure 1 shows the schematic diagram of the flow-through MFC biosensor.

The biosensor was operated at a flow rate of 1 L day^{-1}, corresponding to a hydraulic retention time (HRT) of 2.4 h in the anode compartment. In the experiments, the influent solution components were changed following an experimental design, which included three levels of Cu and two levels of acetate. Acetate concentration in the feed was maintained at 13 mg L^{-1} or 50 mg L^{-1}, while Cu concentration was maintained at either 0, 20 μg L^{-1}, or 200 μg L^{-1}. Therefore, acetate was always fed to the biosensor to maintain the electroactive microbial populations of the anode. The biosensor was operated using the previously described periodic connection of an external resistor (R_{ext}) (Adekunle et al. 2019b). A 470 Ohm external resistor was used throughout the tests. The R_{ext} connection/disconnection algorithm was implemented in MATLAB® software (Mathworks, Natick, MA, USA). The software was modified to estimate parameters of the equivalent circuit model, as explained in the following section. LabJack U3-LV (LabJack Corp., Lakewood, CO, USA) was used for data acquisition at a scan rate of 1000 Hz while the connection/disconnection of R_{ext} was achieved using an ADG801 electronic switch (Analog Devices, Norwood, MA USA).

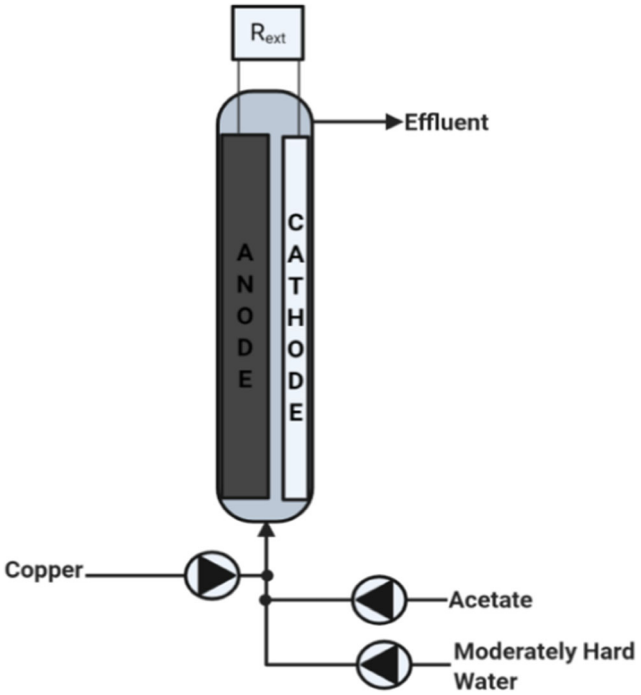

Fig. 1 Schematics of the MFC-based biosensor with carbon felt anode and air-breathing Mn oxide cathode. MHW supplemented with acetate and Cu was continuously fed to the anode compartment bottom

EIS measurements

The electrochemical behavior of the biosensor was characterized by electrochemical impedance spectroscopy (EIS). EIS measurements were carried out in a frequency range of 10 kHz–0.01 Hz at an applied voltage of 0.5 V using the two-electrode configuration (cathode as a reference and counter electrode) to evaluate the overall MFC characteristics. A reference electrode was not used for the tests to minimize disturbances to microbial populations in long-term tests. EIS was performed using a potentiostat/galvanostat analyzer (273A, Princeton Applied Research, USA) controlled by the VersaStudio v2.6 software (Princeton Applied Research, USA). The non-linear least squares (NLLS) fit analysis for EIS data was done using the Zview v3.5 software (Scribner Associates, Inc., USA).

Real-time toxicity estimation

Two approaches for toxicity estimation were implemented. In one approach, the biosensor response was observed based on the steady-state voltages obtained during the periodic connection/disconnection of the R_{ext} (Coronado et al. 2013). The algorithm for determining the steady-state voltage of the biosensor is described in detail elsewhere (Adekunle et al. 2019b). According to this algorithm, at the startup of biosensor operation, R_{ext} is connected, and the biosensor voltage (V_s) is continuously monitored until a steady-state voltage (V_{min}) is observed. Once V_{min} is attained, R_{ext} is disconnected, and the biosensor voltage is monitored again to estimate the open-circuit voltage (V_{max}). The biosensor voltage (V_{min} or V_{max}) is considered to be at a steady state when its variation is less than a predefined small value (ε) for three consecutive data acquisitions. The algorithm is provided in Supplementary Materials, Fig. SI-1.

In the second, soft sensor approach, the biosensor, still operated with the periodic connection of R_{ext}, is described by a simple equivalent circuit model (ECM) with model parameters corresponding to key internal parameters of the MFC, such as internal resistances (R_1, R_2), internal capacitance (C), and open-circuit voltage (V_{oc}). The electrical circuit of the model is shown Supplementary Materials (Fig. SI-2) and described elsewhere (Coronado et al. 2015). When R_{ext} is connected, the voltage dynamics over the internal capacitance, C, can be described by the following first-order differential equation:

$$\frac{dV_c}{dt} = \frac{V_{oc}}{C(R_{ext}+R_1)} - \frac{(R_1+R_2+R_{ext})}{CR_2(R_1+R_{ext})}V_c \tag{1}$$

where V_c is the voltage at the internal capacitor C. If R_{ext} is connected ("on" part of the cycle), Eq. (1) can be solved analytically resulting in the following expressions for V_c and V_{MFC_on} (voltage at R_{ext}) (Coronado et al. 2015):

$$V_c = V_{c,final} + \left(V_{c,0} - V_{c,final}\right)e^{-\frac{(R_1+R_2+R_{ext})}{CR_2(R_1+R_{ext})}t} \tag{2}$$

where $V_{c,0}$ and $V_{c,final}$ are the initial and final voltages at the internal capacitor during the "on" part of each cycle and

$$V_{c,final} = V_{oc}\frac{R_2}{R_1+R_2+R_{ext}} \tag{3}$$

Accordingly,

$$V_{MFC\_on} = \frac{R_{ext}}{R_{ext}+R_1}(V_{oc} - V_c) \tag{4}$$

Also, when R_{ext} is disconnected, the dynamics of the voltage at the biosensor (V_{MFC_off}) can be expressed using the following equations:

$$V_{MFC\_off} = V_{oc} - V_c \tag{5}$$

where

$$V_c = V_{c,final}e^{-\frac{t-t_{on}}{CR_2}} \tag{6}$$

where t_{on} is the "on" time of the cycle during which R_{ext} is connected to the biosensor.

Therefore, the biosensor voltage over one cycle can be expressed as

$$V_s = V_{MFC\_on} + V_{MFC\_off} \tag{7}$$

The ECM parameters are periodically re-estimated using the ECM outputs and a numerical parameter estimation procedure. Changes in the estimated values of model parameters are expected to represent variations in water toxicity. In the experiments, model parameters were estimated with an interval of 1 h.

The internal parameter estimation algorithm used a pulse-width modulated connection of R_{ext} at high and low frequencies, 100 Hz and 0.0008 Hz, respectively, and a duty cycle of 20%. The acquired voltage (V_s) profile was used to estimate the ECM parameters online. Here, R_1 is estimated at the high frequency of R_{ext} connection/disconnection, while V_{oc}, R_2, and C are estimated at the low connection frequency. The parameter estimation was carried out by using the *fminsearch* function in MATLAB to minimize the root mean square error between the experimental V_s profile and a model-based V_{s_m} profile. The V_{s_m} profile is determined by an integration method based on the dynamics of the voltage at the capacitor of the ECM, as described by Eq. (7).

Results and discussion

Biosensor response to changes in Cu and carbon source concentrations

Several previous works have demonstrated successful detection of heavy metal toxicity by MFC biosensors (Adekunle et al. 2019b, 2020; Yi et al. 2019; Yu et al. 2017). The biosensor reacts to the presence of heavy metals due to the changes in the metabolic activity of electroactive microorganisms, which can be observed by estimating the biosensor outputs as well as electrochemical parameters, such as internal resistance and capacitance (Adekunle et al. 2019b; Stein et al. 2012; Yi et al. 2019; Yu et al. 2017). Prolonged exposure to heavy metals also results in microbial population changes, which are well documented (Adekunle et al. 2019b; Kim et al. 2007). In particular, there are several studies on Cu toxicity detection using the MFC biosensor (Adekunle et al. 2020; Jiang et al. 2015; Shen et al. 2013; Zhu and Logan 2014). Accordingly, Cu was chosen as the model toxicant for demonstrating the soft sensor approach for real-time toxicity detection. Experimental work was started by exposing the biosensor to several Cu concentrations. Since carbon source availability is expected to vary in the environment, biosensor response to the presence of Cu was evaluated at two levels of acetate, which served as a carbon source in all experiments.

In the first test, the biosensor response was based on the steady-state voltages obtained during the R_{ext} connection (V_{max}) and disconnection (V_{min}). Also, the anode compartment influent stream contained a constant acetate concentration of 25 mg L^{-1}, while the Cu concentration was progressively increased from 20 to 200 μg L^{-1}. As can be seen from the results of this test (Fig. 2a), the biosensor outputs V_{max} and V_{min} remained relatively constant until a concentration of 100 μg L^{-1} Cu was reached in the influent stream, i.e., at this level of acetate, Cu presence is not detectable by the biosensor if present at less than 100 μg L^{-1}. This Cu detection limit is different from our previous study, where at 35 μg L^{-1} of Cu in lake water, the biosensor voltage (V_{max}) started to decrease (Adekunle et al. 2020). The lower sensitivity to Cu (i.e., higher detection limit) can be attributed to the higher concentration of acetate (carbon source). Indeed, in our previous study, water samples collected from a lake were only spiked with Cu without the addition of acetate, which is the preferred carbon source for several electroactive bacteria, including *Geobacter* spp. (Bond and Lovley 2003; Commault et al. 2016). Lake water typically contains very low levels of readily degradable organic materials. It can be suggested that carbon source availability affects the biosensor sensitivity to metal cations. The protective effect of carbon source was confirmed by increasing acetate concentration up to 75 mg L^{-1} while maintaining a constant level of Cu. As shown in Fig. 2b, with an increase in acetate concentration, both biosensor outputs (V_{max} and V_{min}) also increased. Such linear response to carbon source concentration was observed in a previous study (Gil et al. 2003). Also, the lower sensitivity of anode based

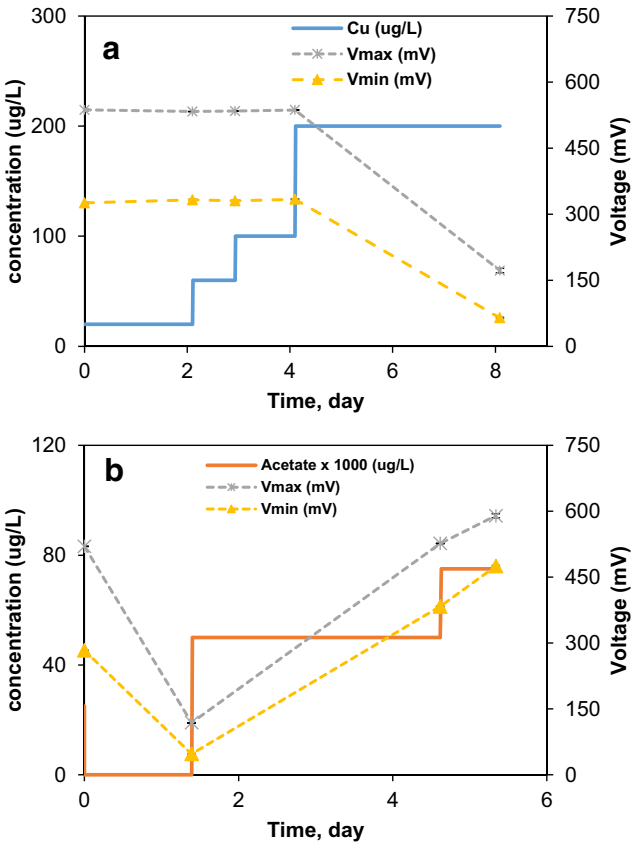

Fig. 2 Biosensor response to changes in **a** Cu and **b** acetate concentration

MFCs in organic matter–rich solutions was documented in several studies (Jiang et al. 2016). Recently, biocathode-based MFC biosensors were proposed to overcome this limitation (Jiang et al. 2017b). Overall, this initial test established the sensitivity limit of the experimental setup at around 100 μg L^{-1} of Cu at the influent acetate concentration of 25 mg L^{-1}.

Equivalent circuit model

The model-based (soft sensor) approach is often used to monitor difficult to measure process parameters, reduce measurement delays, and provide faster detection of process faults (Fortuna et al. 2007). Several MFC models have been proposed, including complex biofilm models (Kato Marcus et al. 2007; Marcus et al. 2007; Picioreanu et al. 2007, 2008; Pinto et al. 2010; Yang and Yang 2020) and much simpler equivalent circuit models (Coronado et al. 2015; Sindhuja et al. 2016) to predict MFC outputs and/or dynamics. While dynamic models are suitable for improving MFC design and operating conditions, the large number of model parameters and their complexity make the use of comprehensive models for monitoring MFC status in real-time applications difficult. On the contrary, a simple equivalent circle model does not provide an adequate description of biomass changes over time and reaction kinetics, but has few parameters, which can be conveniently estimated using either analytical or numerical parameter estimation methods. The simplicity of equivalent circuit models makes them suitable for on-line applications, where fast model solution and the straightforward interpretation of parameter values are essential. Such models can provide qualitative or semi-quantitative estimation of key internal parameters and elucidate performance trends, including response to the presence of toxic compounds. Accordingly, the soft sensor approach in this study was based on using a simple ECM and constantly re-estimating the model parameters in real time according to the algorithm described in the "Material and methods" section.

To select the simplest acceptable ECM structure, a series of EIS tests were carried out at different combinations of Cu and acetate concentrations. Figure 3a shows, as an example, the resulting Nyquist plot obtained from the EIS measurements at 50 mg L^{-1} of acetate and 200 μg L^{-1} of Cu in the influent stream. In the Nyquist plot, two distinctive regions could be seen: a semi-circle at high frequencies and a semi-straight line in the lower frequency region. The semi-circle at high frequencies can be related to the porous structure of the carbon felt anode and the response of the double-layer capacitance. Additionally, it implies that the majority of the electrode's capacitance is reached at low frequencies. On the other hand, at low frequencies, the curve forms a nearly straight line. This effect could be attributed to the contribution of the Faradaic capacitance due to redox reactions occurring at the electrode/electrolyte interface and a slow mass transport of electrons, which is the rate-limiting step (Gomez Vidales et al. 2019a). These EIS measurements were fitted using three equivalent circuit models of varying complexity.

The first tested model, initially proposed by Lepage et al. (2012), accounts for mass transport limitations and the double-layer capacitance (R-CPE-W model). In this model, R_1 represents the ohmic resistance, R_2 and R_3 are the polarization resistances, and CPE1 and CPE2 (constant-phase-elements) represent the double-layer capacitance of the system, where the CPE accounts for the effect of the electrode surface roughness. Also, *W*, the Warburg diffusion element, accounts for mass transport processes, which is the rate-determining step. This model was used for fitting the EIS data in a range of 0.01–10,000 Hz. As can be seen from Fig. 3a, the agreement between the model (solid line) and experimental data (symbols) is excellent. The estimated model parameters are given in Table 1.

Considering that the biosensor does not typically operate at high frequencies and that a simpler model would be easier to implement for real-time applications, the R-CPE-W model was simplified by eliminating the CPE2 and *W* elements. The resulting R-CPE model is shown in Fig. 3b. It comprises R_1, which represents the ohmic resistance; R_2 to account for the polarization resistance; and CPE1, which denotes the double-layer capacitance. The CPE1 element in this model represents the effect of the anode surface roughness (Gomez Vidales et al. 2019b). As can be seen from Fig. 3b, the agreement between the model and the EIS data is acceptable for the reduced range of frequencies.

To further simplify the model, the CPE was replaced with internal capacitance (*C*), as shown in Fig. 3c. Although the resulting R-C model cannot be used for modeling a broad range of frequencies, it was hypothesized that it could provide an acceptable approximation of the EIS results at frequencies less than 100 Hz, which are used for the periodic R_{ext} connection to the biosensor. The resulting model parameters are given in Table 1. This rather simplified model showed the lowest accuracy of data fitting. Nevertheless, the biosensor is typically operated at frequencies lower than 10 Hz, and an acceptable fit of the R-C model for describing MFC dynamics was demonstrated in a previous work (Coronado et al. 2015). This suggests that although the estimated model parameters might be biased, the model is usable for trend estimation in real time.

To evaluate changes in the R-C model parameters, the EIS measurements were performed at four combinations of acetate and Cu concentrations in the influent stream. The Cu concentration was changed between 20 and 200 μg L^{-1}, while acetate concentration changed between 13 and 50 mg L^{-1}. The resulting model parameters are given in Table 2. These results suggest that at 50 mg L^{-1} of acetate, an increase in the Cu concentration decreases internal capacitance and increases internal resistances. This trend is

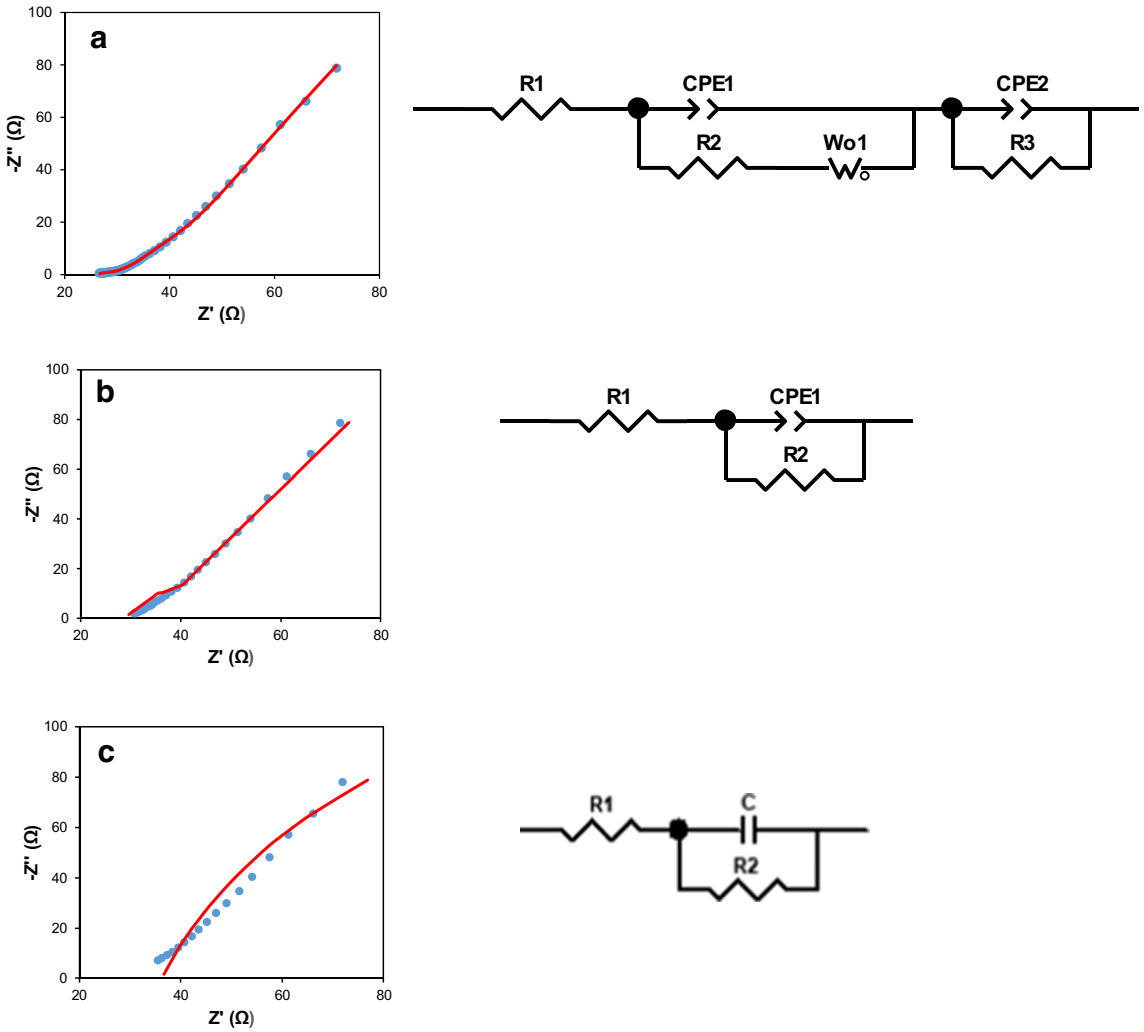

Fig. 3 Nyquist plots of the biosensor and ECM fitting results for the ECM with **a** Warburg diffusion and CPE (R-CPE-W model), **b** R-CPE model, and **c** R-C model. Circuits are shown to the right of each plot. Symbols represent the experimental data and solid lines correspond to the model outputs

Table 1 Parameters obtained for R-CPE-W, R-CPE, and R-C models by fitting EIS measurements recorded at acetate and Cu influent concentrations of 50 mg L^{-1} and 200 μg L^{-1}, respectively. WSR denotes the weighted sum of squared residuals

Parameter	R-CPE-W	R-CPE	R-C
Frequency*	10,000–0.01	10–0.01	1–0.01
R_1 (Ω)	26.11	29.1	39.3
R_2(Ω)	3.79	4.9	23.78
R_3 (Ω)	8.30	–	–
C (F)	–	–	0.16
CPE1 (F s^{n-1})	0.31	0.15	–
n	0.44	0.53	–
CPE2 (F s^{n-1})	0.14	–	–
n	0.66	–	–
W (Ω^{-1} s^{P})	1.35	–	–
P	0.42	–	–
WSR	0.018	0.025	0.47

*Frequency range used for parameter estimation

more pronounced at an influent acetate concentration of 13 mg L^{-1}, i.e., acetate concentration increases *C* values and decreases R_1 and R_2 values. Overall, the impact of Cu concentration is much higher than the impact of acetate. Overall, results presented in Table 2 confirmed that online estimation of the R-C model parameters could be used as an approach for toxicity monitoring.

Table 2 Parameter estimation results for the R-C model in the 100–0.01 Hz frequency range of the biosensor operation during EIS tests. WSR denotes the weighted sum of squared residuals

Parameter	Acetate 50 mg L^{-1}		Acetate 13 mg L^{-1}	
Cu concentration	20 μg L^{-1}	200 μg L^{-1}	20 μg L^{-1}	200 μg L^{-1}
R_1 (Ω)	39.5	41.7	38.6	46.1
R_2 (Ω)	22.6	24.6	21.9	29.2
C (F)	0.19	0.14	0.25	0.11
WSR	0.52	0.49	0.44	0.61

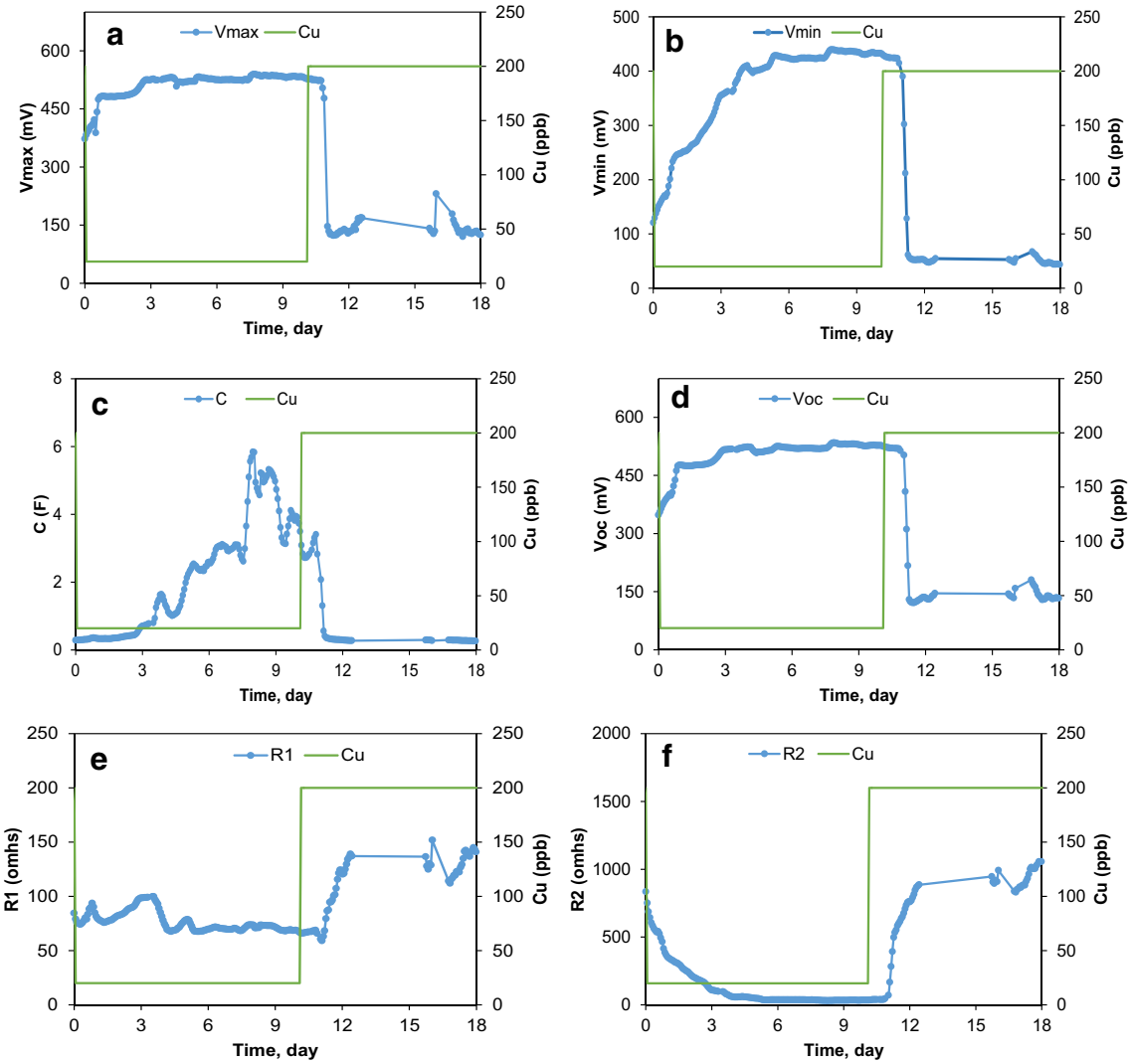

Fig. 4 Changes in simple monitoring parameter (V_{min} and V_{max}) as well as in the ECM parameters (V_{oc}, R_1, R_2, C) during biosensor operation at either 20 or 200 μg L^{-1} of Cu in the influent. At $t = 10$ days, acetate concentration was changed from 50 to 13 mg L^{-1}

Biosensor response to toxicity changes

The results of the electrochemical characterization suggest that while a more detailed R-CPE-W model provides better accuracy, a much simpler R-C model might be sufficient for real-time toxicity detection and monitoring. A previous study (Jiang et al. 2017a), in which an MFC was operated through a transient connection of an external resistor to the MFC, suggested that this model might be sufficient for describing the internal parameters of an MFC biosensor. Notably, in that study, the changes in model parameters were not estimated in real time, and the external resistor connection/disconnection times were pre-set. A connection/disconnection of the resistor based on the attainment of steady state has been shown to be suitable for online toxicity monitoring (Adekunle et al. 2019b). To validate the proposed R-C model-based (soft sensor) approach for online monitoring of the internal parameters during toxicity monitoring, it was compared with the previously described simpler method of V_{max} and V_{min} monitoring. Experiments were carried out at several combinations of acetate and Cu concentrations. The Cu concentration was varied between 20 and 200 μg L^{-1}, while acetate concentration was changed from 50 to 13 mg L^{-1}, as in the previous test. In an additional test, 1000 μg L^{-1} of NaCl was added to the influent stream at the end of the experiment to observe the contribution of water conductivity to MFC response. Overall, these experiments lasted for a total of 36 days.

Prior to the startup of the experiment, the biosensor was operated at an acetate concentration of 13 mg L^{-1} and a Cu concentration of 200 μg L^{-1}. One day before the first test, the concentration of acetate was increased to 50 mg L^{-1}, leading to increasing V_{max} and V_{min} values. Cu concentration was decreased to 20 μg L^{-1}, and the online estimation of changes in the internal parameters of the biosensor was started at $t = 0$. As can be seen from Fig. 4a and b, after the decrease in Cu concentration, both V_{max} and V_{min} were observed to increase. This increase coincided with changes in the model parameters,

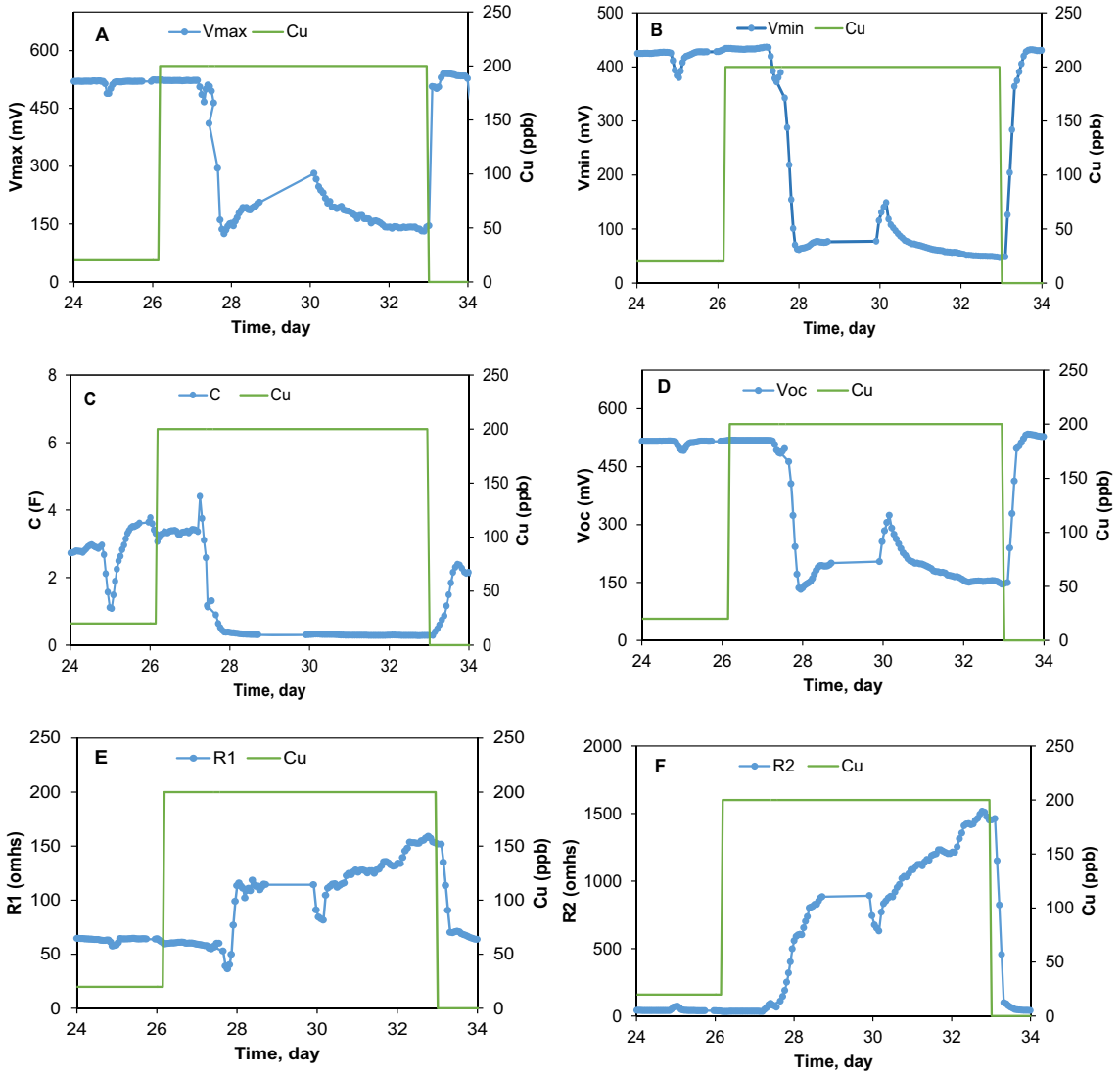

Fig. 5 Changes in simple monitoring parameters (V_{min} and V_{max}) as well as in the ECM parameters (V_{oc}, R_1, R_2, C) during biosensor operation at 0, 20, or 200 μg L^{-1} of Cu in the influent. Acetate concentration maintained at 13 mg L^{-1}

as V_{oc} and C (internal capacitance) progressively increased while R_1 and R_2 decreased, as shown in Fig. 4c–f, respectively. The changes in R_1 (ohmic resistance) were less pronounced than the changes in R_2, suggesting that the impact of changes in the conductivity of the feed stream was minimal.

In general, V_{min} and V_{max} (corresponding to V_{oc}) are directly related to the rate of oxidation at the anode and are expected to be positively correlated with the metabolic activity of electroactive bacteria (Adekunle et al. 2019b). This trend can be different for other internal parameters of the ECM. R_1 and R_2 are associated with ohmic and concentration losses, respectively (Coronado et al. 2015). C is a measure of the electroactive performance of the microbial biofilm at the anode, and V_{oc} is an estimation of the maximum voltage that can be obtained in the system (Coronado et al. 2015). It thus follows that in an MFC with no toxic compounds in the anode compartment, R_1 and R_2 are expected to be low, while C and V_{oc} are expected to increase over time as the microbial biofilm develops, and vice versa. This expectation is confirmed in the model parameters, as shown in Figs. 4a–f. Once Cu concentration was increased to 200 μg L^{-1} at $t = 10$ days, and acetate concentration decreased to 13 mg L^{-1}, a clear drop in V_{max}, V_{min}, V_{oc}, and C values, and an increase in R_1, R_2 values was observed.

In the second test, the acetate concentration was maintained at 13 mg L^{-1}, while Cu concentration was increased from 20 to 200 μg L^{-1} on day 26.2 and then decreased to 0 μg L^{-1} on day 33. As shown in Fig. 5a–f, an increase in Cu concentration above the sensitivity level of the biosensor (100 μg L^{-1}) caused the V_{oc} (V_{max}), V_{min}, and C to decrease and R_1, R_2 to increase. A significant delay of at least 29 h to observe 25% change in each parameter was observed. This delay was shorter for C (29 h), somewhat shorter for V_{min} (about 32 h) and longer for V_{max}, V_{oc}, R_1, and R_2 (40 h). Interestingly, the

Table 3 Results of the online R-C model parameter estimation at several combinations of acetate and Cu concentrations

Parameter	Acetate 50 mg L^{-1}		Acetate 13 mg L^{-1}			
Cu concentration	20 μg L^{-1}	200 μg L^{-1}	0 μg L^{-1}	20 μg L^{-1}	200 μg L^{-1}	200 μg L^{-1} (repeat)
R_1 (Ω)	68.2	91.2	71.95	64.4	166.0	156.9
R_2 (Ω)	34.2	961.33	37.6	40.2	1217.2	1498.3
C (F)	3.8	0.28	2.56	3.2	0.25	0.28
V_{oc} (V)	0.53	0.34	0.52	0.52	0.14	0.15
V_{min} (V)	0.43	0.11	0.43	0.43	0.04	0.05
V_{max} (V)	0.53	0.36	0.53	0.52	0.14	0.14

removal of Cu in the feed on day 33 resulted in a much shorter delay of only 5 h for a 25% change in all parameters. Although there is an obvious delay in changes of biosensor voltage and all internal parameters in response to increased Cu^{2+} concentration, this delay can be mainly attributed to the low concentration of Cu^{2+} used throughout this study. Several previous studies (Jiang et al. 2015; Shen et al. 2013; Zhu and Logan 2014) showed shorter response times at concentrations greater than 1 mg L^{-1}. However, testing MFC biosensor response to concentrations, which are closer to the regulatory limits (typically < 500 μg L^{-1} for most heavy metals), could be more practical. It can be suggested that the response time can be reduced by limiting the supply of organic carbon to the anode compartment, optimizing other operating parameters such as water flow rate, and optimizing the anode compartment design. Finally, feeding 1000 μg L^{-1} of NaCl on day 35–36 (data not shown) to the biosensor did not lead to an observable change in the biosensor's outputs (V_{min} and V_{max}) or the estimated ECM parameters.

Table 3 summarizes steady-state values of the model parameters estimated in real time for different values of acetate and Cu in the influent stream. Altogether, these results confirm the trends observed during the EIS measurements and also suggest that at low carbon source concentrations, electroactive bacteria become more sensitive to changes in dissolved metal concentration. It also appears that with the increase in organic matter availability (e.g., source of electrons), the electrochemical reduction (removal) of metals increases. Subsequently, the microbial biofilm is less exposed to dissolved metals, resulting in reduced sensitivity of the biosensor. This change in metal availability is a plausible explanation of how organic matter availability improves biosensor resilience and reduces sensitivity, as observed in this work and suggested in earlier studies (Adekunle et al. 2019b; Jiang et al. 2017b). It can be suggested that this protective effect also contributes to the delayed response observed in the test. Nevertheless, the detection of toxicity at Cu in the part per billion (ppb) range of concentrations, even with some delay, is still acceptable for real-time toxicity monitoring, especially considering the drawbacks of conventional manual bioassays.

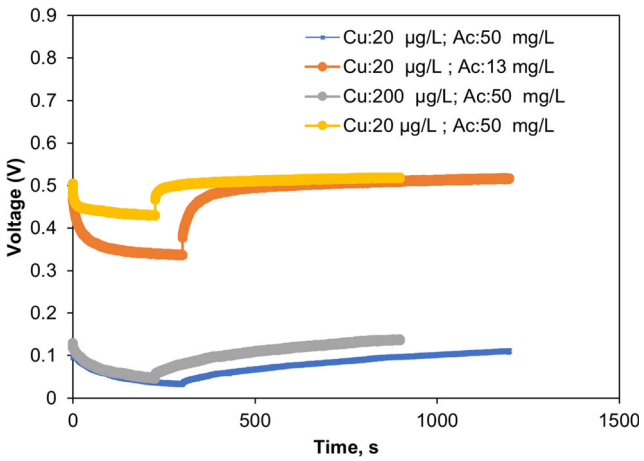

Fig. 6 Changes in the electron transfer rate in MFC-based biosensors due to toxicity

With the on/off mode of operation utilized during this test for biosensor operation, insight into the dynamic response of an MFC-based biosensor was also gained. It is possible to see how the levels of organic matter and toxicants affect the electron transfer rate in the biosensor, as shown in Fig. 6. From the voltage dynamics, it can be seen that at low Cu concentration, the profiles of the biosensor's voltage are similar, irrespective of the acetate concentration in the feed. Conversely, at high Cu concentration, irrespective of the acetate concentration in the feed, the voltage profile changes. This clear distinction in the shape of the profile lends further credibility to the appropriateness of the R-C model parameter estimation as an approach for toxicity detection in real time. In addition, the information obtained by monitoring the biosensor dynamics during on/off operation information implies that there are opportunities for the development of predictive analysis tools that can utilize the voltage profile shape for detecting the onset of toxicity and distinguishing between the carbon source and toxicant impacts.

Conclusions

Although the R-CPE-W model proposed by Lepage et al. (2012) is the most suitable for describing the electrochemical

behavior of the MFC-based biosensor, this study demonstrates that a much simpler R-C model can be used to implement a soft sensor approach for real-time toxicity detection and monitoring. The biosensor in combination with the soft sensor approach can be used for detection and monitoring of Cu-related toxicity, as demonstrated in a series of laboratory tests. Overall, it can be suggested that the model-based approach provides a better chance at timely detecting changes in toxicity levels when compared with a simple voltage monitoring approach proposed in the previous studies (Adekunle et al. 2019b, 2020). The model-based approach should be further exploited for reducing the biosensor response time and for developing algorithms capable of reducing false alarms and biosensor self-diagnostics.

Author contributions AA: methodology, software, investigation, data curation, validation, writing—original draft, writing—review and editing; AGV: methodology, investigation, writing—original draft, writing—review and editing; LW: methodology, validation, investigation, writing—original draft, writing—review and editing; BT: conceptualization, methodology, data curation, writing—original draft, writing—review and editing, funding acquisition.

Data availability Not applicable.

Compliance with ethical standards

Conflict of interest The authors declare that they have no competing interests.

Ethical approval and consent to participate Not applicable.

Consent to publish All the authors have agreed for authorship, read and approved the manuscript and given consent for submission and subsequent publication of the manuscript.

References

Adekunle A, Raghavan V, Tartakovsky B (2019a) A comparison of microbial fuel cell and microbial electrolysis cell biosensors for real-time environmental monitoring. Bioelectrochemistry 126:105–112. https://doi.org/10.1016/j.bioelechem.2018.11.007

Adekunle A, Raghavan V, Tartakovsky B (2019b) On-line monitoring of heavy metals-related toxicity with a microbial fuel cell biosensor. Biosens Bioelectron 132:382–390. https://doi.org/10.1016/j.bios.2019.03.011

Adekunle A, Rickwood C, Tartakovsky B (2020) Online monitoring of heavy metal–related toxicity using flow-through and floating microbial fuel cell biosensors. Environ Monit Assess 192:52

Beauchemin D (2010) Inductively coupled plasma mass spectrometry. Anal Chem 82:4786–4810

Bond DR, Lovley DR (2003) Electricity production by *Geobacter sulfurreducens* attached to electrodes physiology and biotechnology. Appl Environ Microbiol 69:1548–1555. https://doi.org/10.1128/AEM.69.3.1548-1555.2003

Cho J-C et al (2004) A novel continuous toxicity test system using a luminously modified freshwater bacterium. Biosens Bioelectron 20:338–344

Choi S (2015) Microscale microbial fuel cells: advances and challenges. Biosens Bioelectron 69:8–25

Chouler J, Di Lorenzo M (2015) Water quality monitoring in developing countries; can microbial fuel cells be the answer? Biosensors 5:450–470

Chouler J, Cruz-Izquierdo Á, Rengaraj S, Scott JL, Di Lorenzo M (2018) A screen-printed paper microbial fuel cell biosensor for detection of toxic compounds in water. Biosens Bioelectron 102:49–56. https://doi.org/10.1016/j.bios.2017.11.018

Commault AS, Lear G, Bouvier S, Feiler L, Karacs J, Weld RJ (2016) Geobacter-dominated biofilms used as amperometric BOD sensors. Biochem Eng J 109:88–95. https://doi.org/10.1016/j.bej.2016.01.011

Coronado J, Perrier M, Tartakovsky B (2013) Pulse-width modulated external resistance increases the microbial fuel cell power output. Bioresour Technol 147:65–70. https://doi.org/10.1016/j.biortech.2013.08.005

Coronado J, Tartakovsky B, Perrier M (2015) On-line monitoring of microbial fuel cells operated with pulse-width modulated electrical load. J Process Control 35:59–64. https://doi.org/10.1016/j.jprocont.2015.08.004

Fortuna L, Graziani S, Rizzo A et al (2007) Fault detection, sensor validation and diagnosis. In: Fortuna L, Graziani S, Rizzo A et al. (Eds), Soft sensors for monitoring and control of industrial processes. Springer, London. https://doi.org/10.1007/978-1-84628-480-9_9

Gil G-C, Chang I-S, Kim BH, Kim M, Jang J-K, Park HS, Kim HJ (2003) Operational parameters affecting the performannce of a mediator-less microbial fuel cell. Biosens Bioelectron 18:327–334. https://doi.org/10.1016/S0956-5663(02)00110-0

Gomez Vidales A, Kim J, Omanovic S (2019a) Ni 0.6-x Mo 0.4-x Ir x-oxide as an electrode material for supercapacitors: investigation of the influence of iridium content on the charge storage/delivery. J Solid State Electrochem 23:2129–2139

Gomez Vidales A, Omanovic S, Tartakovsky B (2019) Combined energy storage and methane bioelectrosynthesis from carbon dioxide in a microbial electrosynthesis system. Bioresour Technol Rep 8:100302

Gu MB, Gil GC, Kim JH (1999) A two-stage minibioreactor system for continuous toxicity monitoring. Biosens Bioelectron 14:355–361. https://doi.org/10.1016/S0956-5663(99)00017-2

Jiang Y, Liang P, Zhang C, Bian Y, Yang X, Huang X, Girguis PR (2015) Enhancing the response of microbial fuel cell based toxicity sensors to Cu(II) with the applying of flow-through electrodes and controlled anode potentials. Bioresour Technol 190:367–372. https://doi.org/10.1016/j.biortech.2015.04.127

Jiang Y et al (2016) Enhancing signal output and avoiding BOD/toxicity combined shock interference by operating a microbial fuel cell sensor with an optimized background concentration of organic matter. Int J Mol Sci 17:1392

Jiang Y, Liang P, Liu P, Miao B, Bian Y, Zhang H, Huang X (2017) Enhancement of the sensitivity of a microbial fuel cell sensor by transient-state operation. Environ Sci Water Res Technol 3:472–479

Jiang Y, Liang P, Liu P, Wang D, Miao B, Huang X (2017b) A novel microbial fuel cell sensor with biocathode sensing element. Biosens Bioelectron 94:344–350

Jiang Y, Liang P, Huang X, Ren ZJ (2018) A novel microbial fuel cell sensor with a gas diffusion biocathode sensing element for water and air quality monitoring. Chemosphere 203:21–25. https://doi.org/10.1016/j.chemosphere.2018.03.169

Kato Marcus A, Torres CI, Rittmann BE (2007) Conduction-based modeling of the biofilm anode of a microbial fuel cell. Biotechnol Bioeng 98:1171–1182

Kholodkevich S, Ivanov A, Kurakin A, Kornienko E, Fedotov V (2008) Real time biomonitoring of surface water toxicity level at water supply stations. Environ Bioindic 3:23–34

Kim M, Sik Hyun M, Gadd GM, Joo Kim H (2007) A novel biomonitoring system using microbial fuel cells. J Environ Monit 9:1323–1328. https://doi.org/10.1039/b713114c

Lee JH, Gu MB (2005) An integrated mini biosensor system for continuous water toxicity monitoring. Biosens Bioelectron 20:1744–1749

Lepage G, Albernaz FO, Perrier G, Merlin G (2012) Characterization of a microbial fuel cell with reticulated carbon foam electrodes. Bioresour Technol 124:199–207. https://doi.org/10.1016/j.biortech.2012.07.067

Logroño W, Guambo A, Pérez M, Kadier A, Recalde C (2016) A terrestrial single chamber microbial fuel cell-based biosensor for biochemical oxygen demand of synthetic rice washed wastewater. Sensors 16:101

Marcus A, Torres CI, Rittmann BE (2007) Conduction-based modeling of the biofilm anode of a microbial fuel cell. Biotechnol Bioeng 98:1171–1182

Pham TTP, Nguyen PHD, Nguyen TTV, Duong HTL (2019) Self-build packed-bed bioreactor for rapid and effective BOD estimation. Environ Sci Pollut Res 26:25656–25667. https://doi.org/10.1007/s11356-019-05711-z

Picioreanu C, Head IM, Katuri KP, van Loosdrecht MC, Scott K (2007) A computational model for biofilm-based microbial fuel cells. Water Res 41:2921–2940

Picioreanu C, Katuri K, Head I, van Loosdrecht MC, Scott K (2008) Mathematical model for microbial fuel cells with anodic biofilms and anaerobic digestion. Water Sci Technol 57:965–971

Pinto R, Srinivasan B, Manuel M-F, Tartakovsky B (2010) A two-population bio-electrochemical model of a microbial fuel cell. Bioresour Technol 101:5256–5265

Rabaey KVW (2005) Microbial fuel cells: novel biotechnology for energy generation trends in biotechnology. Trends Biotechnol 23:291–298

Recio-Garrido D, Adekunle A, Perrier M, Raghavan V, Tartakovsky B (2017) Wastewater Treatment and Online Chemical Oxygen Demand Estimation in a Cascade of Microbial Fuel Cells. Ind Eng Chem Res 56:12471–12478. https://doi.org/10.1021/acs.iecr.7b02586

Schievano A, Colombo A, Cossettini A, Goglio A, D'Ardes V, Trasatti S, Cristiani P (2018) Single-chamber microbial fuel cells as on-line shock-sensors for volatile fatty acids in anaerobic digesters. Waste Manag 71:785–791. https://doi.org/10.1016/j.wasman.2017.06.012

Shen Y, Wang M, Chang IS, Ng HY (2013) Effect of shear rate on the response of microbial fuel cell toxicity sensor to Cu(II). Bioresour Technol 136:707–710. https://doi.org/10.1016/j.biortech.2013.02.069

Sindhuja M, Kumar NS, Sudha V, Harinipriya S (2016) Equivalent circuit modeling of microbial fuel cells using impedance spectroscopy. J Energy Storage 7:136–146

Stein NE, Hamelers HMV, Van Straten G, Keesman KJ (2012) On-line detection of toxic components using a microbial fuel cell-based biosensor. J Process Control 22:1755–1761. https://doi.org/10.1016/j.jprocont.2012.07.009

Wang D, Liang P, Jiang Y, Liu P, Miao B, Hao W, Huang X (2018) Open external circuit for microbial fuel cell sensor to monitor the nitrate in aquatic environment. Biosens Bioelectron 111:97–101. https://doi.org/10.1016/j.bios.2018.04.018

Wu Q, Jiao S, Ma M, Peng S (2020) Microbial fuel cell system: a promising technology for pollutant removal and environmental remediation. Environ Sci Pollut Res 27:6749–6764. https://doi.org/10.1007/s11356-020-07745-0

Xu X, Ying Y (2011) Microbial biosensors for environmental monitoring and food analysis. Food Rev Int 27:300–329

Yang Z, Yang A (2020) Modelling the impact of operating mode and electron transfer mechanism in microbial fuel cells with two-species anodic biofilm. Biochem Eng J 158:107560. https://doi.org/10.1016/j.bej.2020.107560

Yi Y, Xie B, Zhao T, Li Z, Stom D, Liu H (2019) Effect of external resistance on the sensitivity of microbial fuel cell biosensor for detection of different types of pollutants. Bioelectrochemistry 125:71–78. https://doi.org/10.1016/j.bioelechem.2018.09.003

Yu D, Bai L, Zhai J, Wang Y, Dong S (2017) Toxicity detection in water containing heavy metal ions with a self-powered microbial fuel cell-based biosensor. Talanta 168:210–216

Zhao T, Xie B, Yi Y, Liu H (2019) Sequential flowing membrane-less microbial fuel cell using bioanode and biocathode as sensing elements for toxicity monitoring. Bioresour Technol 276:276–280. https://doi.org/10.1016/j.biortech.2019.01.009

Zhou S, Huang S, Li Y, Zhao N, Li H, Angelidaki I, Zhang Y (2018) Microbial fuel cell-based biosensor for toxic carbon monoxide monitoring. Talanta 186:368–371. https://doi.org/10.1016/j.talanta.2018.04.084

Zhu X, Logan BE (2014) Copper anode corrosion affects power generation in microbial fuel cells. J Chem Technol Biotechnol 89:471–474. https://doi.org/10.1002/jctb.4156